Looking for the Charged Higgs Boson at LHC[1]

D.P. Roy

Tata Institute of Fundamental Research
Homi Bhabha Road, Mumbai 400 005, India

I discuss LHC signatures of the charged Higgs boson of the MSSM, focussing mainly on the case of the $H^{\pm}$ being heavier than top quark.

The minimal supersymmetric Standard Model (MSSM) contains two complex Higs doublets, ϕ_1 and ϕ_2, corresponding to eight scalar states. Three of these are absorbed as Goldstone bosons leaving five physical states – the two neutral scalars (h^0, H^0), a pseudo-scalar (A^0) and a pair of charged Higgs bosons $(H^{\pm})$. All the tree-level masses and couplings of these particles are given in terms of two parameters, $m_{H^{\pm}}$ and $\tan\beta$, the latter representing the ratio of the two vacuum expectation values [1]. While any one of the above neutral Higgs bosons may be hard to distinguish from that of the Standard Model, the $H^{\pm}$ carries a distinctive hall-mark of the SUSY Higgs sector. Moreover the couplings of the $H^{\pm}$ are uniquely related to $\tan\beta$, since the physical charged Higgs boson corresponds to the combination

$$H^{\pm} = -\phi_1^{\pm} \sin\beta + \phi_2^{\pm} \cos\beta. \qquad (1)$$

Therefore the detection of $H^{\pm}$ and measurement of its mass and couplings are expected to play a very important role in probing the SUSY Higgs sector.

The $t \to bH^+$ decay is known to provide promising signatures for charged Higgs boson search at TEVATRON upgrade and LHC for $M_H < m_t$ [2]. But it is hard to extend the $H^{\pm}$ search beyond m_t, because in this case the combination of dominant production and decay channels, $tH^- \to t\bar{t}b$, suffers from a large QCD background [3]. Moreover the subdominant

---

[1]Invited talk at the Cairo International Conference on High Energy Physics, 9-14 January 2001.

production channels of $H^\pm W^\mp$ and $H^\pm H^\mp$ have been found to give no viable signature at LHC [4]. In view of this we have undertaken a systematic study of a heavy $H^\pm$ signature at LHC from its dominant production channel $tH^-(\bar{t}H^+)$, followed by the decays $H^- \to \bar{t}b, \tau\bar{\nu}$ and W^-h^0. While the 1st represents the dominant decay channel of charged Higgs boson, the $\tau\nu$ and Wh^0 are the largest subdominant channels in the high and low $\tan\beta$ regions respectively, with

$$B_{\tau\nu}(\tan\beta \gtrsim 10) \sim 15\% \quad \text{and} \quad B_{Wh^0}(\tan\beta = 1-5) \lesssim 5\%. \tag{2}$$

The signature for the dominant decay channel of $H^- \to \bar{t}b$ has been analysed separately assuming three and four b-tagging. The analyses are generally based on parton level Monte Carlo program with gaussian smearing of lepton and jet momenta for simulating detector resolution.

(i) $H^\pm \to tb$ Signature with Four b-tags [5]:

The dominant signal and background processes are

$$gg \to tH^-\bar{b} + \text{h.c.} \to t\bar{t}b\bar{b}, \tag{3}$$

$$gg \to t\bar{t}b\bar{b}, \tag{4}$$

followed by the leptonic decay of one top and hadronic decay of the other, i.e.

$$t\bar{t}b\bar{b} \to b\bar{b}b\bar{b}W^+W^- \to b\bar{b}b\bar{b}\ell\nu q\bar{q}. \tag{5}$$

A basic set of kinematic and isolation cuts,

$$p_T > 20 \text{ GeV}, \ |\eta| < 2.5, \ \Delta R = \left[(\Delta\phi)^2 + (\Delta\eta)^2\right]^{1/2} > 0.4 \tag{6}$$

is imposed on all the jet and lepton momenta. The p_T cut is also imposed on the missing-p_T, obtained by vector addition of the p_T's after resolution smearing. This is followed by the mass reconstruction of the W and the top quark pair, so that one can identify the pair of b-jets accompanying the latter. While the harder of these two b-jets (b_1) comes from $H^\pm$ decay in the signal, both of them come mainly from gluon splitting in the background. Consequently the S/B ratio is improved by imposing the following cuts on this b-jet pair:

$$M_{bb} > 120 \text{ GeV}, \ E_{b_1} > 120 \text{ GeV} \quad \text{and} \quad \cos\theta_{bb} < 0.75. \tag{7}$$

Then each of this b-jet pair is combined with each of the reconstructed pair of top to give 4 entries for the invariant mass M_{tb} per event. One of these 4 entries corresponds to the $H^\pm$ mass for the signal event, while the others constitute a combinatorial background. Fig. 1 shows this tb invariant mass distribution for the signal (3) and background (4). The right hand scale corresponds to the cross-section for $\epsilon_b^4 = 0.1$ – i.e. an optimistic b-tagging efficiency of $\epsilon_b = 0.56$. Reducing it to a more conservative value of $\epsilon_b = 0.4$ would reduce both the signal and background by a factor of 4 each.

Table 1. Number of signal and background events
in the 4 b-tagged channel per 100 fb^{-1} luminosity
in a mass window of $M_{H^\pm} \pm 40$ GeV at
$\tan\beta = 40$ ($\epsilon_b = 0.4$).

$M_{H^\pm}$(GeV)	S	B	$S/\sqrt{B}$
310	32.7	26.9	6.3
407	22.7	17.3	5.5
506	13.2	9.9	4.2
605	7.5	5.5	3.2

Table 1 lists the number of signal and background events for a typical annual luminosity of 100 fb^{-1}, expected from the high luminosity LHC run, assuming $\epsilon_b = 0.4$. While the S/B ratio is > 1, the viability of the signal is limited by the signal size[2]. One expects a $> 3\sigma$ signal upto $M_{H^\pm} = 600$ GeV at $\tan\beta = 40$. The signal size is very similar at $\tan\beta = 1.5$, but smaller in between. The reason the extreme values of $\tan\beta$ are favoured is that the signal process (3) is controlled by the $tbH^\pm$ Yukawa coupling,

$$\frac{g}{\sqrt{2}M_W}H^+\left[\cot\beta m_t \bar{t}b_L + \tan\beta m_b \bar{t}b_R\right], \tag{8}$$

which is large for $\tan\beta \sim 1$ and $\sim m_t/m_b$. Interestingly these two regions of $\tan\beta$ are favoured by $b - \tau$ unification for a related reason: i.e. one needs a large $tbH^\pm$ Yukawa coupling contribution to the RGE to control the rise of m_b as one goes down from the GUT to the low energy scale [6].

(ii) $H^\pm \to tb$ Signature with Three b-tags [7]:

The contributions to this signal come from (3) as well as

$$gb \to tH^- + \text{h.c.} \to t\bar{t}b + \text{h.c.}, \tag{9}$$

followed by the leptonic decay of one top and hadronic decay of the other. The signal cross-section from (9) is 2-3 times larger than from (3), while their kinematic distributions are very similar. Combining the two and subtracting the overlapping piece to avoid double counting [8] results in a signal cross-section, which is mid-way between the two. The background comes from (4) as well as

$$gb \to t\bar{t}b + \text{h.c.} \quad \text{and} \quad gg \to t\bar{t}g, \tag{10}$$

---

[2]Increasing the p_T cut of b-jets from 20 to 30 GeV would reduce the signal (background) size by a factor of about 3(4), hence reducing the viability of this signal.

3

where the gluon jet in the last case is mis-tagged as a b-jet. Assuming the standard mistagging factor of 1% this contribution turns out in fact to be the largest source of the background, as we see below.

The basic kinematic cuts are as in (6) except for a harder p_T-cut, $p_T > 30$ GeV, since the 3 b-jets coming from $H^\pm$ and $t\bar{t}$ decays are all reasonably hard. This is followed by the mass reconstruction of the top quark pair as before, so that one can identify the accompanying (3rd) b-jet. We impose a $p_T > 80$ GeV cut on this b-jet to improve the S/B ratio. Finally this b-jet is combined with each of the reconstructed top pair to give two entries of M_{tb} per event. One of them corresponds to the $H^\pm$ mass for the signal while the other constitutes the combinatorial background. Fig. 2 shows this tb invariant mass distribution of the signal along with the above mentioned backgrounds, including a b-tagging efficiency factor of $\epsilon_b = 0.4$. While the S/B ratio is < 1 the signal cross-section is much larger than the previous case. Table 2 lists the number of signal and background events for a luminosity of 100 fb^{-1} at $\tan\beta = 40$. The results are very similar at $\tan\beta = 1.5$. Comparing this with Table 1 we see that the $S/\sqrt{B}$ ratio is very similar in the two channels. One should bear in mind however the larger p_T cut assumed for the 3 b-tagged channel. The cross-sections in both the cases were calculated with the MRS-LO structure functions [9].

Table 2. Number of signal and background events
in the 3 b-tagged channel per 100 fb^{-1} luminosity
in a mass window of $M_{H^\pm} \pm 40$ GeV at
$\tan\beta = 40$ ($\epsilon_b = 0.4$).

$M_{H^\pm}$ (GeV)	S	B	$S\sqrt{B}$
310	133	443	6.2
407	111	403	5.6
506	73	266	4.5
605	43	156	3.4

(iii) $H^\pm \to \tau\nu$ Signature [10]:

For simplicity we have estimated the signal and background cross-sections from

$$gb \to tH^- + \text{h.c.} \to b\bar{q}q\tau\bar{\nu} + \text{h.c.} \tag{11}$$

$$gg \to t\bar{t} \to b\bar{q}q\bar{b}\tau\bar{\nu} + \text{h.c.} \tag{12}$$

followed by the 1-prong hadronic decay of τ. The signal contains a hard a positively polarized τ, while the background contains a relatively soft and negatively polarized τ from W boson decay. The polarization difference can be exploited to sharpen the signal by simply requiring the charged pion to carry $> 80\%$ of the visible τ momentum. Fig. 3 shows the signal and background cross-sections against the transverse mass of the τ-jet with the missing-p_T. We see that by exploiting the polarization difference one can get a clean $H^\pm$ signal in this channel for the large $\tan\beta$ region at the level of a few fb. This has been recently confirmed by a more detailed simulation by the CMS collaboration including detector acceptance [11].

(iv) $H^\pm \to W^\pm h^0$ Signature [12]:

We have estimated the signal cross-section from

$$gb \to tH^- + \text{h.c.} \to bW^+W^-h^0 + \text{h.c.,} \tag{13}$$

followed by $h^0 \to b\bar{b}$, $W^\pm \to \ell\nu$ and $W^\mp \to q\bar{q}$. Thus the final state consists of the same particles as the dominant decay mode of eq. (9). Therefore we have to consider the background from the $H^- \to t\bar{b}$ decay (9) along with those from the QCD processes of eq. (10).

We require 3 b-tags along with the same basic cuts as in section (ii). This is followed by the mass reconstruction of $W^\pm$ and the top, which helps to identify the accompanying b-pair and the W. The resulting bb and Wb invariant masses are then subjected to the constraints,

$$M_{bb} = m_{h^0} \pm 10 \text{ GeV and } M_{Wb} \neq m_t \pm 20 \text{ GeV.} \tag{14}$$

The h^0 mass constraint and the veto on the second top helps to distinguish the $H^\pm \to W^\pm h^0$ signal from the backgrounds. However the former is severely constrained by the signal size as well as the S/B ratio. Consequently one expects at best a marginal signal in this channel and that too only in a narrow strip of the $M_{H^\pm} - \tan\beta$ parameter space, at the boundary of the LEP exclusion region. Fig. 4 shows the signal (13) along with the backgrounds from (9) and (10) against the reconstructed $H^\pm$ mass at one such point – $M_{H^\pm} = 220$ GeV and $\tan\beta = 2$.

The LEP limit of $m_{h_0}(m_{A_0}) > 100$ GeV in the low $\tan\beta$ region implies that the $H^\pm \to Wh^0(WA^0)$ decay channel has as high a threshold as the $t\bar{b}$ channel, while the latter has a more favourable coupling. Consequently the $H^\pm \to Wh^0(WA^0)$ decay BR is restricted to be $\lesssim 5\%$ over the LEP allowed region [13]. However the LEP constraint does not hold in singlet extensions of the MSSM like the NMSSM [14]. Consequently the $H^\pm \to Wh^0(WA^0)$ can be the dominant decay mode for $M_{H^\pm} \sim 160$ GeV in the low $\tan\beta$ region and lead to a spectacular signal at the LHC, as is illustrated in [12]. One needs a systematic analysis of the LHC signatures for both neutral and charged Higgs bosons in the NMSSM, particularly in the low $\tan\beta$ region.

It should be mentioned here that these parton level Monte Carlo analyses of the $H^\pm$ signature in tb and Wh^0 decay channels need to be followed up by detailed simulation with PYTHIA, including detector acceptance, as in the case of the $\tau\nu$ channel [11]. Finally it should be noted that practically all the analyses of $H^\pm$ signal so far are based on the lowest order production vertex, represented by the Yukawa coupling of eq. (8). One loop

electroweak corrections to this vertex can give upto 10 (20)% reduction in the signal cross-section at high (low) $\tan\beta$, as recently shown in [15]. The corresponding correction from QCD loops is expected to be larger, but not yet available. This is evidently important for a quantitative evaluation of this signal. One should also bear in mind the possibility of a large correction to this vertex from SUSY loops depending on the choice of SUSY parameters [16].

References

[1] J.F. Gunion, H.E. Haber, G.L. Kane and S. Dawson, *"The Higgs Hunters' Guide"* (Addison-Wesley, Reading, MA, 1990).

[2] S. Raychaudhuri and D.P. Roy, *Phys. Rev.* D **52**, 1556 (1995) and D **53**, 4902 (1996); E. Ma, D.P. Roy and J. Wudka, *Phys. Rev. Lett.* **80**, 1162 (1998).

[3] V. Barger, R.J.N. Phillips and D.P. Roy, *Phys. Lett.* B **324**, 236 (1994); J.F. Gunion, *Phys. Lett.* B **322**, 125 (1994).

[4] A.A. Barrientos Bendezú and B.A. Kniehl, *Phys. Rev.* D **59**, 015009 (1999) and hep-ph/9908385; S. Moretti and K. Odagiri, *Phys. Rev.* D **59**, 055008 (1999).

[5] D.J. Miller, S. Moretti, D.P. Roy and W.J. Stirling, *Phys. Rev.* D **61**, 055011 (2000).

[6] V. Barger, M.S. Berger and P. Ohmann, *Phys. Rev.* D **47**, 1093 (1993).

[7] S. Moretti and D.P. Roy, *Phys. Lett.* B **470**, 209 (1999).

[8] F. Borzumati, J.-L. Kneur and N. Polonsky, *Phys. Rev.* D **60**, 115011 (1999); D. Dicus, T. Stelzer, Z. Sullivan and S. Willenbrock, *Phys. Rev.* D **59**, 094016 (1999).

[9] A.D. Martin, R.G. Roberts, W.J. Stirling and R.S. Thorne, *Phys. Lett.* B **443**, 301 (1998).

[10] D.P. Roy, *Phys. Lett.* B **459**, 607 (1999).

[11] R. Kinnunen, Higgs working group report for the *Les Houches Workshop* on *Physics at TeV Colliders*, hep-ph/0002258, pp 46-48.

[12] M. Drees, M. Guchait and D.P. Roy, *Phys. Lett.* B **471**, 39 (1999).

[13] S. Moretti and W.J. Sterling, *Phys. Lett.* B **347**, 291 (1995), Erratum, *ibid*, B **366**, 451 (1996); A. Djouadi, J. Kalinowski and P.M. Zerwas, *Z. Phys.* C **70**, 435 (1996).

[14] M. Drees, E. Ma, P.N. Pandita, D.P. Roy and S. Vempati, *Phys. Lett.* B **433**, 346 (1998).

[15] L.G. Jin, C.S. Li, R.J. Oakes and S.H. Zhu, hep-ph/9907482.

[16] J.A. Coarasa, D. Garcia, J. Guasch, R.A. Jimenez and J. Sola, *Eur. Phys. J.*, C **2**, 373 (1998).
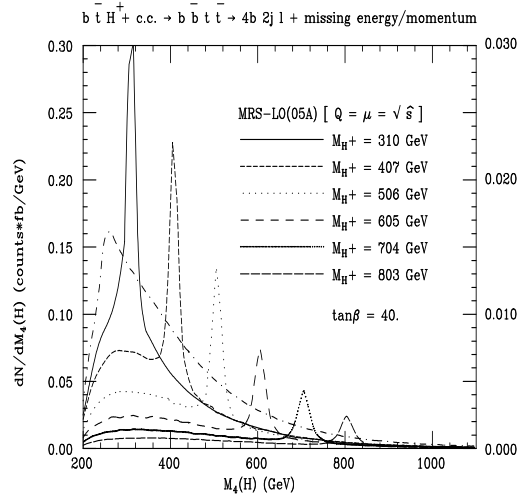
Fig. 1. The reconstructed tb invariant mass distribution of the $H^{\pm}$ signal (3) and the QCD background (4) in the isolated lepton plus multi-jet channel with 4 b-tags. The scale on the right corresponds to a b-tagging efficiency fator $\epsilon_b^4 = 0.1$.
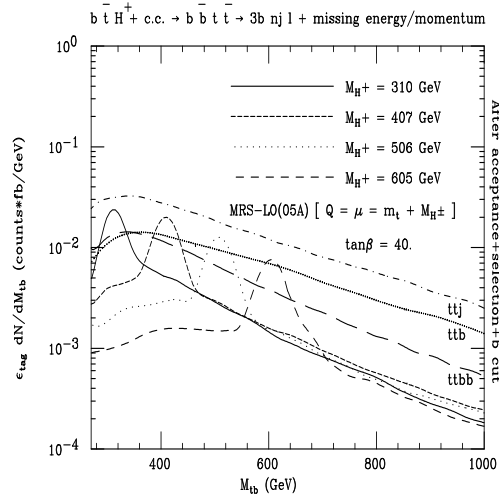

Fig. 2. The reconstructed tb invariant mass distribution of the $H^{\pm}$ signal and different QCD backgrounds in the isolated lepton plus multijet channel with 3 b-tags.
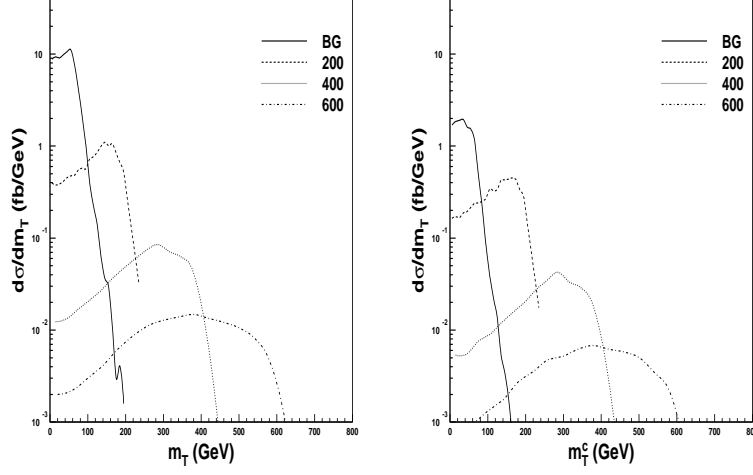
Fig. 3. Distribution of the $H^\pm$ signal and background cross-sections in the transverse mass of the τ-jet with the missing-p_T for (a) all 1-prong τ-jets, (b) those where the charged pion carries over 80% of the τ-jet p_T ($M_{H^\pm} = 200, 400, 600$ GeV and $\tan\beta = 40$).
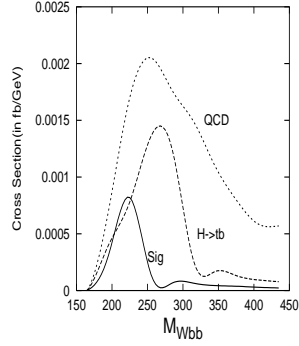

Fig. 4. The $H^\pm \to W h^0$ signal cross-section is shown against the reconstructed $H^\pm$ mass for $M_{H^\pm} = 220$ GeV and $\tan\beta = 2$ along with the $H^\pm \to tb$ and the QCD backgrounds.